Global NEST Journal, Vol 19, No 4, pp 716-725

Effect of flow and module configuration on SO_2 absorption by using membrane contactors

Zhang Z.[1,2,3,*], Zhao S.[1], Rezakazemi M.[4], Chen F.[2], Luis P.[5] and Van der Bruggen B.[6]

[1]School of Chemistry and Chemical Engineering, Chongqing University of Technology, Chongqing 400054, China

[2]Fujian Provincial Key Laboratory of Featured Materials in Biochemical Industry, Ningde Normal University, Ningde 352100, China

[3]Key Laboratory of Low-grade Energy Utilization Technologies and Systems, Ministry of Education of China, Chongqing University, Chongqing 400044, China

[4]Department of Chemical and Materials Engineering, Shahrood University of Technology, Shahrood, Iran

[5]Materials & Process Engineering (iMMC-IMAP), Université catholique de Louvain, 1348 Louvain-la-Neuve, Belgium

[6]Department of Chemical Engineering, ProcESS, KU Leuven, W. de Croylaan 46, B-3001 Leuven, Belgium

Received: 13/02/2017, Accepted: 02/01/2018, Available online: 17/01/2018

*to whom all correspondence should be addressed: e-mail: zhienzhang@hotmail.com

Abstract

Sulfur dioxide (SO_2) emissions lead to negative environmental impacts and it is considered as an indicator for the larger group of gaseous sulfur oxides (SO_x) in the air. In this paper, the dimethylamine (DMA) solution was used as the absorbent in a α-Al_2O_3 hollow fiber membrane contactor that is operated under several conditions of gas velocity, liquid velocity, and 290 K operating temperature. The effects of gas and liquid phase properties and module configuration on SO_2 absorption efficiency in the hollow fiber membrane contactor were investigated. Simulation results showed that the changes of gas phase velocity, liquid phase velocity, and concentration have great influences on the absorption efficiency of SO_2. An increase of the gas flow rate decreases the SO_2 absorption efficiency, while an increase of the liquid flow rate has the opposite effect, increasing the efficiency. Because gas in the membrane module stays for a longer time, more absorption time promotes the gas and liquid reaction. However, the changes of the volume fraction of SO_2 in the mixed gas are not significant to SO_2 absorption. The simulation model could provide guidelines for selecting suitable fluid properties during the SO_2 absorption process in a hollow fiber membrane contactor.

Keywords: SO_2 Absorption; Hollow fiber membrane; Gas and liquid phases; Absorption efficiency; Numerical modelling

1. Introduction

Currently, fossil fuels (such as coal, oil, and natural gas) are the primary energy sources throughout the world. As a result, fuel combustion will continue to emit sulfur dioxide (SO_2) and nitrogen oxides (NO_x) at an astonishing annual rate. In addition, SO_2 emissions lead to acid rain, air pollution, urban smog, and harm to human health and ecosystems (Rahmani *et al.*, 2015; Bokotko *et al.*, 2005). Thus, it is very urgent to remove SO_2 from air. Currently, there are several common methods for SO_2 removal, i.e., wet scrubbing (Jin *et al.*, 2006; Andreasen *et al.*, 2007), dry scrubbing (Neather, 1996), and wet sulfuric acid process (Kikkawa *et al.*, 2002). But there are some shortcomings using these approaches, i.e., foaming, entrainment, flooding, and channeling issues, and a large required space (Mansourizadeh *et al.*, 2010). Membrane gas absorption (MGA) is an effective way for SO_2 removal which provides a large gas and liquid contact surface and a high packing density using a hollow fiber membrane contactor. In addition, the membrane only acts as a fixed interface while gases transport takes place across the membrane. Gas and

liquid can be operated separately using the contactor (Park *et al.*, 2007).

The MGA method was first employed in gas absorption in 1985 by Qi and Cussler (1985). The gas and liquid system was operated without flooding problems even at high gas flow rates. This was due to the indirect contact between gas and liquid. CO_2 capture using MGA method has been a popular topic and widely investigated (Zhang *et al.*, 2014, 2014a; Zhang, 2016). However, there were a few publications reported on the membrane absorption process of SO_2 (Park *et al.*, 2007; Luis *et al.*, 2010; Yu *et al.*, 2016).

Karoor and Sirkar, (1993) carried out SO_2 absorption experiments in pure water in a packed tower and a hollow fiber contactor. They found that efficient contacting was achieved in the case of a hollow fiber membrane contactor when compared to conventional reactors. In addition, the K_La value using MGA was around 10 times higher than that using conventional methods. Park *et al.* (Park *et al.*, 2008) performed a series of SO_2 absorption experiments in a polyvinylidenefluoride (PVDF) hollow fiber membrane. A variety of absorbents including NaOH, Na_2CO_3, Na_2SO_3, and $NaHCO_3$ solutions were compared regarding the SO_2 absorption performance. It was proved that the Na_2CO_3 solution showed the best performance for SO_2 absorption. Most previous studies have focused on experimental research and a few modeling works have been conducted (Luis *et al.*, 2010; Yu *et al.*, 2016; Fasihi *et al.*, 2012). Yu *et al.* (2016) proposed a model for SO_2 absorption into water accompanied with reversible reaction in a hollow fiber membrane contactor and investigated the effects of inlet SO_2 concentration and temperature on the membrane performance. In our previous work (Zhang *et al.*, 2015), the effects of membrane and contactor geometry parameters on SO_2 absorption performance were studied theoretically. The proposed model could provide guidelines for selecting the optimum contactor parameters.

The purpose of this current work is to focus on the fluid dynamic properties and module configuration influences on SO_2 absorption efficiency in a hollow fiber membrane. The governing equations for material balances in three sections, i.e., the tube, membrane, and shell sides, were calculated and solved with the given boundary conditions. Three-dimensional concentration schematic is presented with different fluid dynamic parameters. The developed model could provide guidelines for selecting optimal fluids properties during SO_2 absorption process in a hollow fiber membrane contactor.

2. Hollow fiber membrane contactor

Figure 1 (a) shows a physical model of SO_2 absorption inside a hollow fiber membrane contactor. A mixed gas containing SO_2 and air entered into the module and reacted with the absorbent of dimethylamine (DMA). Figure 1 (b) describes the SO_2 transport process inside the hollow fiber membrane contactor.

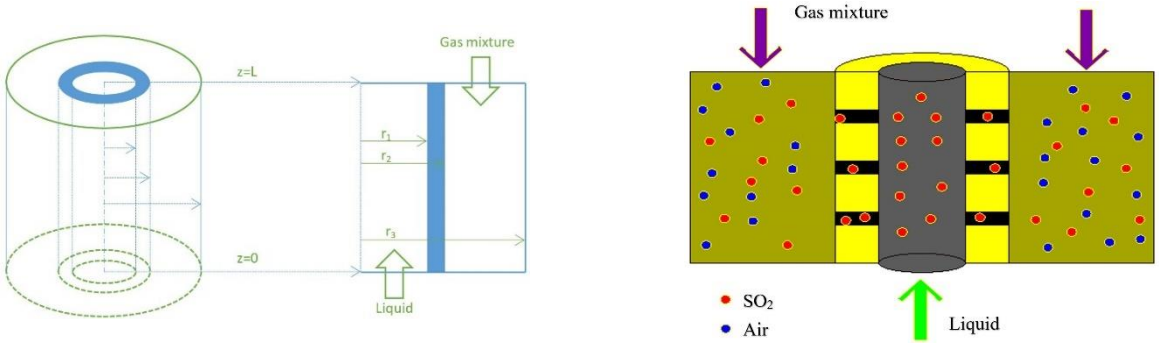

(a) (b)

Figure 1. Hollow fiber membrane absorbing SO_2: (a) the internal structure and (b) gas and liquid flows

The mixed gas flowed out of the hollow fibers (shell side), and the absorbent flowed on the other side of the membrane contactor (tube side). Meanwhile, SO_2 was absorbed into the absorbent in the tube side to complete the desulfurization after mixed gas entered into the membrane fibers. When gas and liquid were operated under the ideal conditions, the model could be simplified to the process of a hollow fiber absorbing SO_2. Mixed gas

with 5% SO_2 and air is considered under the conditions of 0.1 L min^{-1} gas flow rate and 1 L min^{-1} liquid flow rate.

3. Numerical Model

In this case, some assumptions are made to simplify the mass continuity equations for calculating the developed model:

1. The liquid phase in the tube is a steady flowing fluid under the isothermal condition, with stable physical properties, and the liquid velocity distribution in the tube presents a parabolic curve;
2. The effect of the axial diffusion and radial convective mass transfer is neglected;
3. The gas in the shell side is an ideal gas, and the fluid inside the tube is a Newtonian-type fluid;
4. Both the velocity distribution and the concentration distribution in the tube are axisymmetric;
5. The solute at the gas-liquid phase contact surface follows Henry's law.

3.1. The control equation of membrane

Since the membrane is hydrophobic, the SO_2 transport is considered in the non-wetted condition. Thus, the governing equation can be expressed as:

$$-D_{SO_2\text{-}M}\nabla\cdot\left(\nabla C_{SO_2\text{-}M}\right)=0 \quad (1)$$

where $C_{SO_2\text{-}M}$ is the SO_2 concentration, and $D_{SO_2\text{-}M}$ is SO_2 diffusion coefficient in the membrane which can be written as:

$$D_{SO_2\text{-}M}=D_{SO_2\text{-}L}(\varepsilon/\tau) \quad (2)$$

where ε and τ represent the porosity and tortuosity of the used membrane material, respectively. The boundary conditions within the membrane domain are as follows:

$$\text{at } r = r_1,\ C_{SO_2\text{-}M}=C_{SO_2\text{-}L}/m \quad (3)$$

$$\text{at } r = r_2,\ C_{SO_2\text{-}M}=C_{SO_2\text{-}G} \quad (4)$$

$$\text{at } z = 0, L,\ \partial C_{SO_2\text{-}M}/\partial z =0 \quad (5)$$

where r_1 and r_2 are the inner and outer radii of fiber membrane, respectively. The third boundary condition means that both sides of the membrane section in the axial direction are impermeable.

3.2. The control equation of shell side

The steady state continuity equation of SO_2 flowing in the shell side can be expressed using Fick's law to estimate the diffusion flux, as follows:

$$-D_{SO_2\text{-}G}\nabla\cdot\left(\nabla C_{SO_2\text{-}G}\right)+\nabla\cdot\left(C_{SO_2\text{-}G}V_{z\text{-}G}\right)=0 \quad (6)$$

where $D_{SO_2\text{-}G}$ and $C_{SO_2\text{-}G}$ denote the diffusion coefficient and the concentration of SO_2 in the gas phase, respectively. $V_{z\text{-}G}$ represents the velocity of SO_2 inside the shell side in the z direction.

Assuming the principle of Happel free surface model, the radius of free surface can be expressed as (J. Viscous., 1959):

$$r_e=r_2\sqrt{\frac{1}{\theta}} \quad (7)$$

where r_e is the radius of Happel free surface, and θ represents packed density of the membrane contactor.

The axial velocity within the shell side can be expressed as (Zhang *et al.*, 2015):

$$V_{z\text{-}G}=2V_{av\text{-}G}\left[1-\left(\frac{r_2}{r_3}\right)^2\right]\left[\frac{(r/r_3)^2-(r_2/r_3)^2+2\ln(r_2/r)}{3+(r_2/r_3)^4-4(r_2/r_3)^2+4\ln(r_2/r_3)}\right] \quad (8)$$

The boundary conditions inside the shell side are:

$$\text{at } r=r_2,\ C_{SO_2\text{-}G}=C_{SO_2\text{-}M} \quad (9)$$

$$\text{at } r=r_e,\ \partial C_{SO_2\text{-}G}/\partial r=0 \text{ (symmetric)} \quad (10)$$

$$\text{at } z=L,\ C_{SO_2\text{-}G}=C_0 \quad (11)$$

where C_0 is the initial concentration of SO_2 in the feed gas.3.3. The control equation of tube side

The steady state continuity equation in the tube side can be represented as:

$$-D_{SO_2\text{-}L}\nabla\cdot\left(\nabla C_{SO_2\text{-}L}\right)+\nabla\cdot\left(C_{SO_2\text{-}L}V_{z\text{-}L}\right)=R_{SO_2} \quad (12)$$

where $D_{SO_2\text{-}L}$ and $C_{SO_2\text{-}L}$ represent the diffusion coefficient, and the concentration of SO_2 in liquid phase, respectively. In addition, $V_{z\text{-}L}$ and R_{SO_2} denote the z-velocity of the inner tube and the gas-liquid reaction rate, respectively.

Assuming that the flow velocity inside the tube side is at a fully developed laminar flow state, the flow velocity distribution can be written as (Zhang *et al.*, 2015):

$$V_{z\text{-}L}=2V_{av\text{-}L}\left[1-\left(\frac{r}{r_1}\right)^2\right] \quad (13)$$

where $V_{av\text{-}L}$ is the average velocity in the z direction and r_1 is the inner radius of the hollow fiber membrane. The boundary conditions within the tube side can be expressed as:

$$\text{at } r = r_1, \quad C_{SO_2\text{-}L}=mC_{SO_2\text{-}M} \tag{14}$$

$$\text{at } z = 0, \quad C_{SO_2\text{-}L}=0, \quad C_{L\text{-}T}=C_{initial} \tag{15}$$

$$\text{at } r = 0, \quad \partial C_{SO_2\text{-}L}/\partial r =0 \ \text{(symmetric)} \tag{16}$$

where m is the dimensionless Henry coefficient between gas and liquid phases, $C_{initial}$ is the initial concentration of the absorbent.

3.4. Reaction mechanisms

3.4.1 The reaction mechanism between SO_2 and water

The chemical reaction between SO_2 and water is (Roberts *et al.*, 1980):

$$SO_2+2H_2O \overset{k_1}{\Leftrightarrow} H_3O^++HSO_3^- \quad k_E=0.014 \text{ mol m}^{-3} \tag{17}$$

$$HSO_3^-+H_2O \overset{k_2}{\Leftrightarrow} H_3O^++SO_3^{2-} \quad k_E'=6.24\times10^{-8} \text{ mol m}^{-3} \tag{18}$$

where both k_E and k_E' are equilibrium constants. When the solution pH is lower than 4-5, the formation of SO_3^{2-} can be neglected. If the concentration of HSO_3^- is the same as H_3O^+, the solution presents electrically neutral, and the expression of reaction rate can be written as:

$$-R_{SO_2}=k_1C_{SO_2}-\frac{k_1}{k_E}\left(C_{HSO_3^-}\right)^2 \tag{19}$$

where the SO_2 ionization rate constant (k_1) is 3.17×10^{-2} s^{-1}.

3.4.2 The reaction mechanism between SO_2 and DMA

In the chemical reaction between SO_2 and DMA, the following chemical reactions occur:

$$SO_2+H_2O \Leftrightarrow H^++HSO_3^- \tag{20}$$

$$HSO_3^- \Leftrightarrow H^++SO_3^{2-} \tag{21}$$

$$DMA+H^+ \Leftrightarrow DMAH^+ \tag{22}$$

Besides, it is possible to produce extra chemical product during the chemical reaction between SO_2 and DMA. The chemical equation is (Basu and Dutta, 1987):

$$SO_2+C_6H_5N(CH_3)_2 \Leftrightarrow C_6H_5N(CH_3)_2\cdot SO_2 \tag{23}$$

The reaction between the gas and liquid phases is not only an instantaneous reaction but also a reversible reaction at high DMA concentrations. And the pseudo-first-order reaction rate constant could be found in literature.

3.5. The model numerical solution method

The parameters of the hollow fiber membrane contactor in this paper are presented in Table 1.

Table 1. Parameters of hollow fiber membrane contactor (Luis *et al.*, 2008).

Parameter	Symbol	Value
Fiber materials		α-Al_2O_3
Canning material		316 stainless steel
Packing material		Epoxide resin
Fiber outside diameter (μm)	d_o	4000
Fiber inside diameter (μm)	d_i	3000
Fiber length (m)	L	0.44
Fiber number	n	280
Effective membrane contact area (m^2)	S	0.8
Fiber pore size (nm)	d_p	100

The finite element method using COMSOL Multiphysics software was applied in the numerical solution of the control equations in the developed model. The numerical solver UMFPACK is mainly used in meshing error control. It is a promote format of implicit time and is applied to solve the nonlinear, rigid and stiff boundary, which is also a good two-dimensional model numerical solver. The computer configuration of numerical simulation is a 64-bit operating system, with a 4.00GB memory space and Inter core AMD A8-4500M APU. Furthermore, Table 2 presents the physical and chemical properties of SO_2 as well as liquid absorbent, and reactive kinetic parameters between two phases. Figure 2 is the schematic diagram of triangular mesh

elements in the hollow fiber membrane contactor. The software generates a series of isotropic triangular grid with a triangle smallest unit and creates cells according to a certain proportion. There are 24156 grids in this figure. Meanwhile, the area with dense meshes means large changes in the fluid concentration. This is due to that the absorbent inside the tube side reacting with SO_2.

Table 2. Diffusion coefficient and Henry's coefficient of SO_2 and DMA

Name	Parameter	Number	Reference
Henry's coefficient between SO_2 and water	$m_{SO_2\text{-}H_2O}$	25.86	Hikita *et al.*, 1977
Diffusion coefficient between SO_2 and water ($m^2\ s^{-1}$)	$D_{SO_2\text{-}H_2O}$	2×10^{-9}	Dutta *et al.*, 1987
Henry's coefficient between SO_2 and DMA solution	$m_{SO_2\text{-}DMA}$	0.00131	Koonaphapdeelert *et al.*, 2009
Diffusion coefficient between SO_2 and DMA solution ($m^2\ s^{-1}$)	$D_{SO_2\text{-}DMA}$	2.1×10^{-9}	Bird *et al.*, 2002
SO_2 diffusion coefficient in the gas mixture ($m^2\ s^{-1}$)	$D_{SO_2\text{-}Gas}$	1.26×10^{-5}	Luis *et al.*, 2010

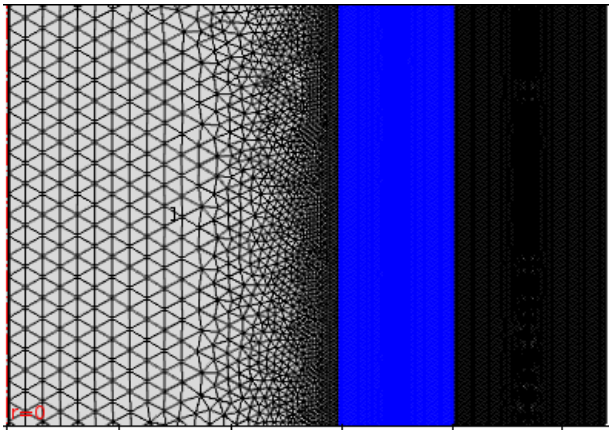

Figure 2. Schematic diagram of triangular mesh element in the membrane contactorResults and discussion

4.1 Concentration distributions

The visual description of the SO_2 concentration distribution inside the membrane contactor with three-dimensional concentration schematic is presented in Figures 3 (a-f). They showed the SO_2 three-dimensional concentration inside the membrane contactor when reacting with 2 mol L^{-1} DMA solution at various gas velocities, respectively. As observed, the SO_2 concentration in the shell side of the membrane contactor gradually decreased from 2.0 to 1.06, 1.23, 1.35, 1.43, 1.48, and 1.53 mol L^{-1}. It was obvious that SO_2 in the mixed gas reacted continually with the DMA solutions, resulting in the continuous decrease in SO_2 concentration at the exit of the shell side. Figure 4 describes the concentration changes of SO_2 in the hollow fiber membrane. Its variation trend was similar to the changes of SO_2 in shell side, decreasing from z=L to z=0. According to Figure 5, the SO_2 concentration in the liquid phase increases from z=0 to z=L. This was due to the DMA solution absorbed SO_2 in the tube, and then the SO_2 concentration at the exit of tube reached to the highest value. Due to the concentration gradient of SO_2 between the tube and membrane sides, the SO_2 concentration gradually reduced from the interface between the tube and membrane sides to the central axis of the membrane contactor.

4.2 Effect of the gas flow velocity (model verification)

Figure 6 demonstrates the comparison between the simulation results of SO_2 removal efficiency and the experimental data reported in the literature (Luis *et al.*, 2010; Shirazian *et al.*, 2011) at different gas velocities.

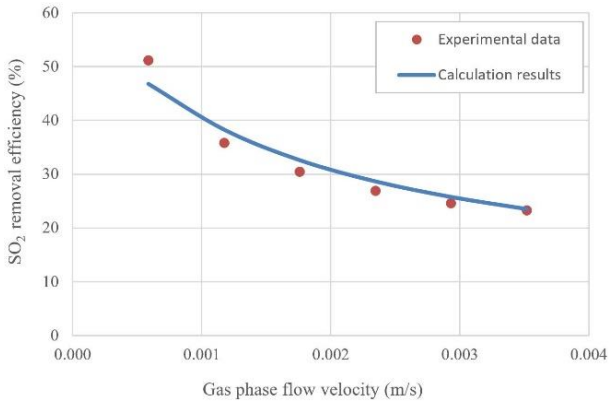

Fig. 6 Effect of the gas phase velocity on SO_2 absorption efficiency (mixed gas of 5% SO_2 and air, the liquid phase flow rate is 1 L min^{-1}, the operating temperature is 290K).

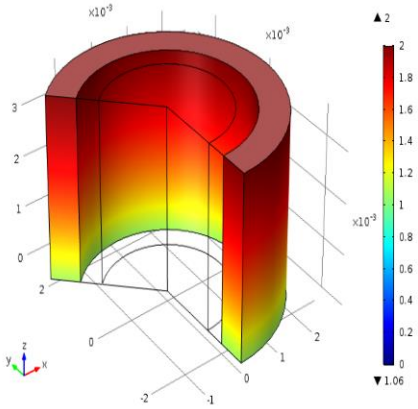

(a)

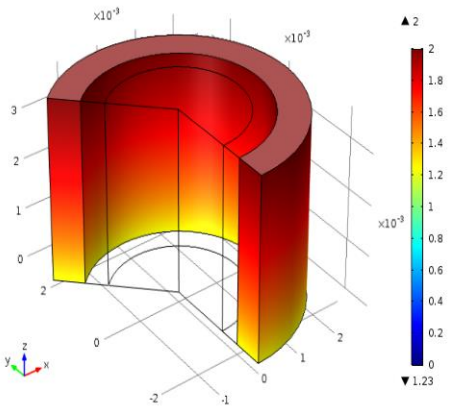

(b)

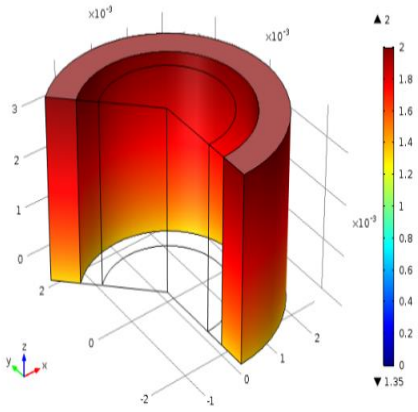

(c)

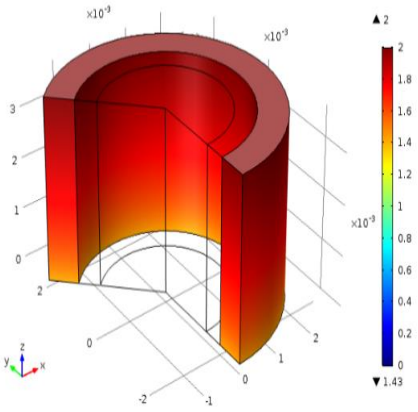

(d)

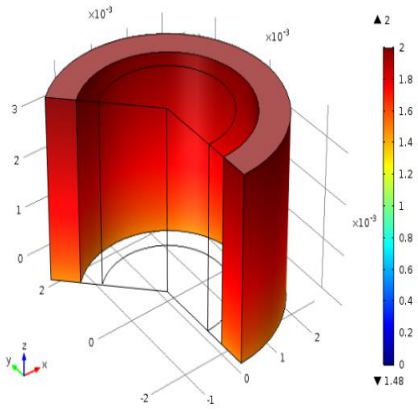

(e)

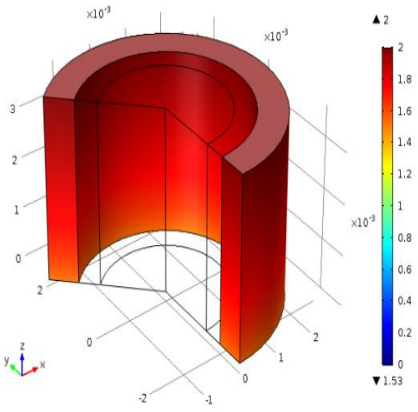

(f)

Figure 3. The three-dimensional concentration distribution of SO_2 reacting with DMA in the shell side (mixed gas of 5% SO_2 and air, the liquid phase flow rate is 1 L min^{-1}, the operating temperature is 290 K. V_g represents the gas phase flow velocity, a: V_g=0.0006 m s^{-1}; b: V_g=0.0012 m s^{-1}; c: V_g=0.0018 m s^{-1}; d: V_g=0.0023 m s^{-1}; e: V_g=0.0029 m s^{-1}; and f: V_g=0.0035 m s^{-1})

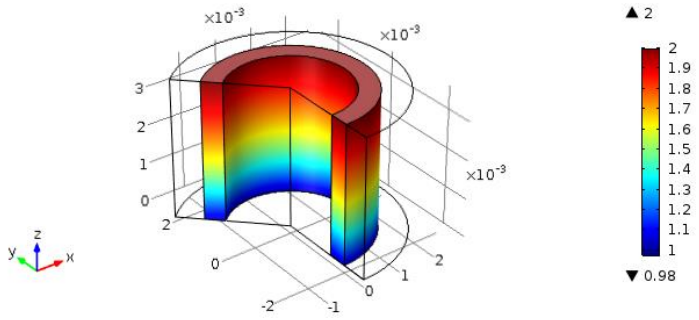

Figure 4. The SO_2 concentration distribution in the hollow fiber membrane contactor (mixed gas of 5% SO_2 and air, the liquid phase flow rate is 1 L min^{-1}, the gas phase flow rate is 0.1 L min^{-1}, the operating temperature is 290 K)

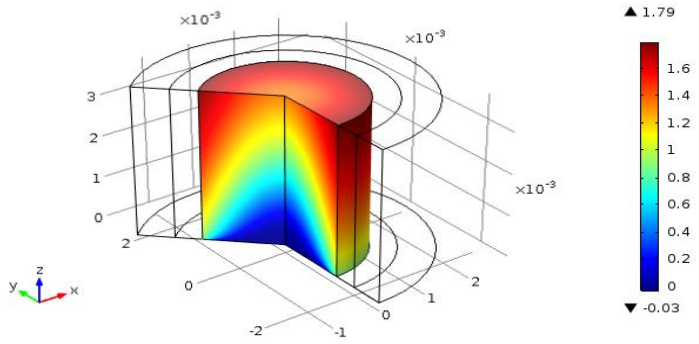

Figure 5. The three-dimensional concentration distribution diagram of the SO_2 concentration in tube side (mixed gas of 5% SO_2 and air, the gas phase flow rate is 0.1 L min^{-1}, the liquid phase flow rate is 1 L min^{-1}, the operating temperature is 290 K)

It can be seen from this figure that when the gas velocity increased from 0.0006 to 0.0035 m s^{-1}, SO_2 removal efficiency dramatically decreased from 46.82 to 23.5%. The reason was that when the velocity of gas phase increased, the gas and liquid reaction time reduced significantly. Although the SO_2 removal efficiency was high with a low gas velocity, the mass transfer effect of the whole process was relatively poor. The conclusion in literature (Eslami *et al.*, 2011; Faiz *et al.*, 2009) had a similar result trend. Figure 7 shows the influence of the gas phase velocity on SO_2 flux. As the gas velocity increased from 0.0006 to 0.0035 m s^{-1}, the absorbed flux of SO_2 decreased from 0.522 to 0.261 mol m^{-2} h^{-1}. Thus, it was necessary to consider comprehensively the influence of the gas velocity on the removal efficiency and the mass transfer rate of SO_2 while selecting the optimal gas velocity conditions of the system.

4.3 Effect of the liquid phase velocity

The influence of the liquid phase velocity on SO_2 removal efficiency was examined from 0.0042 to 0.2528 m s^{-1} using a 2 mol L^{-1} DMA solution. As shown in Figure 8, the removal efficiency increases constantly with increasing the liquid-phase flow velocity. This was because that with the increment in the liquid phase velocity, the disturbance of the liquid in the tube enhanced, and the thickness of boundary layer and the resistance for the liquid mass transfer decreased.

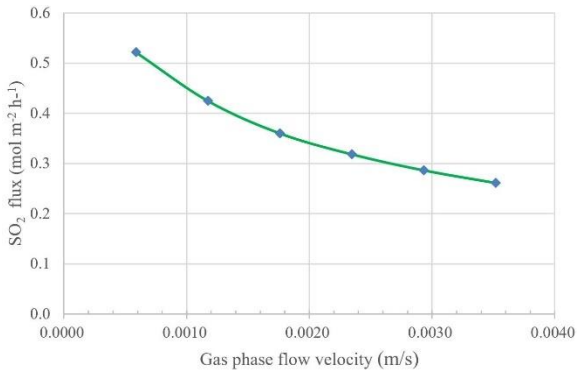

Fig. 7 Effect of the gas phase velocity on SO_2 flux (mixed gas of 5% SO_2 and air, the liquid phase flow rate is 1 L min^{-1}, the operating temperature is 290K).

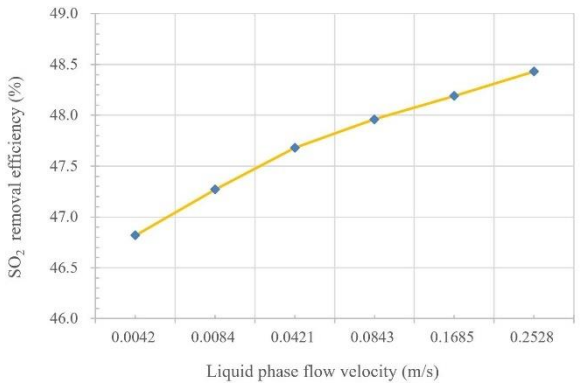

Fig. 8 Effect of the liquid phase velocity on SO_2 absorption efficiency (mixed gas of 5% SO_2 and air, the gas-phase flow rate is 0.1 L min^{-1}, the operating temperature is 290K).

Therefore, this was conductive to the uniform distribution of the liquid, and more fresh DMA solutions could react with SO_2 which finally improved the SO_2 removal efficiency. Although increasing the liquid phase velocity promoted the SO_2 absorption process, it was possible to increase the membrane wettability and the mass transfer resistance which deteriorated the absorption process. Thus, the liquid phase velocity should be controlled during the process of SO_2 absorption. This can not only avoid the wettability issue of the membrane to some extent, but also reduce the energy consumption in the process of SO_2 absorption.

4.4 Effect of SO_2 volume fraction

Table 3 demonstrates the influence of SO_2 volume fraction in the gas mixture on the removal efficiency. It was noted that the SO_2 removal efficiency remained around 46.82% while the SO_2 concentration increased from 0.15 to 4.8%. Therefore, in this case, the change in SO_2 volume fraction in mixed gas only had a slight effect on the SO_2 absorption efficiency within a certain range. Because under the given operating conditions of the experiment system, SO_2 content in the gas mixture was much less than air content and there was no obvious effect on the whole removal process.

Table 3. The results of SO_2 absorption efficiency with different SO_2 volume fractions in the gas mixture (The gas phase velocity is 0.1 L min^{-1}, the liquid phase velocity is 1 L min^{-1}, the operating temperature is 290 K).

SO_2 volume fraction (%)	**SO_2 absorption efficiency (%)**
0.15	46.83
0.30	46.83
0.60	46.82
2.40	46.82
3.30	46.82
4.80	46.81

4.5 Effect of the number of the membrane contactors

In some cases, SO_2 absorption performance for a single membrane contactor was limited, increasing the number of the hollow fiber membrane contactor had a positive effect on SO_2 absorption. This was because considering the membrane contactors in series, the gas and liquid contact area increased and the gas and liquid reaction time in the contactor was longer (Zhang *et al.*, 2017, 2018). Thus, the SO_2 absorption efficiency improved.

Table 4 demonstrates the changes of SO_2 absorption efficiency in the cases of single and serial membrane contactors. The results revealed that the absorption efficiency using the membrane contactors in series was about 20% higher than that of for single one. However, in the actual production application, serial membrane contactors increased the investment and installation costs, and more space were needed for placing the membrane contactors. Furthermore, when selecting an optimal membrane contactor, the influences of the absorption efficiency and the lowest cost shoule be comprehensively considered.

Table 4. Comparisons of SO_2 absorption efficiency with various numbers of the membrane contactor (mixed gas of 5% SO_2 and air, the liquid phase flow rate is 1 L min^{-1}, the operating temperature is 290 K).

Gas velocity (m s^{-1})	**SO_2 removal efficiency for a single membrane contactor (%)**	**SO_2 removal efficiency for the serial membrane contactors (%)**
0.0006	46.82	63.15
0.0012	38.30	61.95
0.0018	32.60	54.50

4. Conclusions

Regarding the atmospheric pollution caused by SO_2, this paper uses a promising method of membrane absorption. The effect of the gas and liquid flows properties and the module configuration on SO_2 absorption was investigated numerically.

In this study, a three-dimensional distribution of SO_2 concentration in the hollow fiber membrane contactor was observed visually by applying a CFD model. The distribution of SO_2 concentration was shown intuitively with changing the gas and liquid phase parameters. Then, the model validation was carried out between the experimental data and the simulation results at different gas flow velocities. It showed that the developed model was feasible and reliable. The simulation results indicated that as increasing the gas phase velocity or SO_2 volume fraction in the gas mixture, the SO_2 absorption efficiency presented a descending tendency; as increasing the liquid phase velocity, SO_2 removal efficiency showed an upward tendency; as considering the membrane contactors in series, the SO_2 removal efficiency increased apparently. Finally, this model could efficiently predict the influence of the gas and liquid parameters and the module configuration on SO_2 absorption, which could optimize the system data and provide guidelines for the operation of the actual application in the future.

Acknowledgements

The authors would like to acknowledge the financial support from Open Funds of Key Laboratory of Low-grade Energy Utilization Technologies and Systems, Ministry of Education of China (LLEUTS-201708, LLEUTS-201307) and Fujian Provincial Key Laboratory of Featured Materials in Biochemical Industry (FJKL_FMBI201704), Scientific and Technological Research Program of Chongqing Municipal Education Commission (KJ1709193, KJ1500940), and Scientific Research Fund of Chongqing University of Technology (2016ZD07).

Nomenclature

D diffusion coefficient ($m^2\ s^{-1}$)

V velocity ($m\ s^{-1}$)

C concentration ($mol\ m^{-3}$)

k reaction rate constant ($m^3\ mol^{-1}\ s^{-1}$)

m solubility

p membrane pore

r radial distance (μm)

R overall reaction rate ($mol\ m^{-3}\ s^{-1}$)

T temperature (K)

ε membrane porosity

τ tortuosity factor

Subscripts

av average

G gas phase

L liquid phase

M membrane

T tube

References

Andreasen A. and Mayer S. (2007), Use of seawater scrubbing for SO_2 removal from marine engine exhaust gas, *Energy & Fuels*, **21**, 3274-3279.

Basu R.K. and Dutta B.K. (1987), Kinetics of absorption of sulfur dioxide in dimethylaniline solution, *The Canadian Journal of Chemical Engineering,* **65**, 27-35.

Bokotko R.P., Hupka J., and Miller J.D. (2005), Flue gas treatment for SO_2 removal with air-sparged hydrocyclone technology, *Environmental Science & Technology,* **39**, 1184-1189.

Bird R.B., Stewai W.E. and Lightfoot E.N. (2002), Transport Phenomena, Second Edition, John Wiley & Sons, Inc, New York.

Dutta B.K., Basu R.K., Pandit A. and Ray P. (1987), Absorption of sulfur dioxide in citric acid-sodium citrate buffer solutions, *Industrial & Engineering Chemistry Research,* **26**, 1291-1296.

Eslami S., Mousavi S.M., Danesh S. and Banazadeh H. (2011), Modeling and simulation of CO_2 removal from power plant flue gas by PG solution in a hollow fiber membrane contactor, *Advances in Engineering Software,* **42**, 612-620.

Faiz R. and Al-Marzouqi M. (2009), Mathematical modeling for the simultaneous absorption of CO_2 and H_2S using MEA in hollow fiber membrane contactors, *Journal of Membrane Science,* **342**, 269-278.

Fasihi M., Shirazian S., Marjani A. and Rezakazemi M. (2012), Computational fluid dynamics simulation of transport phenomena in ceramic membranes for SO_2 separation, *Mathematical and Computer Modelling,* **56**, 278-286.

Happel J. (1959), Viscous flow relative to arrays of cylinders, *AIChE Journal,* **5**, 174-177.

Hikita H., Asai S. and Tsuji T. (1977), Absorption of sulfur dioxide into aqueous sodium hydroxide and sodium sulfite solutions, *AIChE Journal,* **23**, 538-544.

Jin D.S., Deshwal B.R., Park Y.S. and Lee H.K. (2006), Simultaneous removal of SO_2 and NO by wet scrubbing using aqueous chlorine dioxide solution, *Journal of Hazardous Materials,* **135**, 412-417.

Karoor S. and Sirkar K.K. (1993), Gas absorption studies in microporous hollow fiber membrane modules, *Industrial & Engineering Chemistry Research,* **32**, 674-684.

Kikkawa H., Nakamoto T., Morishita M. and Yamada K. (2002), New wet FGD process using granular limestone, *Industrial & Engineering Chemistry Research,* **41**, 3028-3036.

Koonaphapdeelert S., Wu Z. and Li K. (2009), Carbon dioxide stripping in ceramic hollow fibre membrane contactors, *Chemical Engineering Science,* **64**, 1-8.

Luis P., Garea A. and Irabien A. (2010), Modelling of a hollow fibre ceramic contactor for SO_2 absorption, *Separation and Purification Technology,* **72**, 174-179.

Luis P., Garea A. and Irabien A. (2008), Sulfur dioxide non-dispersive absorption in N, N-dimethylaniline using a ceramic membrane contactor, *Journal of Chemical Technology & Biotechnology,* **83**, 1570-1577.

Mansourizadeh A., Ismail A.F. and Matsuura T. (2010), Effect of operating conditions on the physical and chemical CO_2 absorption through the PVDF hollow fiber membrane contactor, *Journal of Membrane Science,* **353**, 192-200.

Neathery J.K. (1996), Model for flue-gas desulfurization in a circulating dry scrubber, *AIChE Journal,* **42**, 259-268.

Park H.H., Lim C.W., Jo H.D., Choi W.K. and Lee H.K. (2007), Absorption of SO_2 using PVDF hollow fiber membranes with PEG as an additive, *Korean Journal of Chemical Engineering,* **24**, 693-697.

Park H., Deshwal B., Kim I. and Lee H. (2008), Absorption of SO_2 from flue gas using PVDF hollow fiber membranes in a gas–liquid contactor, *Journal of Membrane Science,* **319**, 29-37.

Qi Z. and Cussler E.L. (1985), Microporous hollow fibers for gas absorption: I. Mass transfer in the liquid, *Journal of Membrane Science,* **23**, 321-332.

Rahmani F., Mowla D., Karimi G., Golkhar A. and Rahmatmand B. (2015), SO_2 removal from simulated flue gas using various aqueous solutions: Absorption equilibria and operational data in a packed column, *Separation and Purification Technology,* **153**, 162-169.

Roberts D.L. and Friedlander S.K. (1980), Sulfur dioxide transport through aqueous solutions: Part I. Theory, *AIChE Journal,* **26**, 593-602.

Shirazian S., Marjani A. and Azizmohammadi F. (2011), Prediction of SO_2 transport across ceramic membranes using Finite Element Method (FEM), *Oriental Journal of Chemistry,* **27**, 485-490.

Yu, H., Thé J., Tan Z. and Feng X. (2016), Modeling SO_2 absorption into water accompanied with reversible reaction in a hollow fiber membrane contactor, *Chemical Engineering Science,* **156**, 136-146.

Zhang Z. (2016), Comparisons of various absorbent effects on carbon dioxide capture in membrane gas absorption (MGA) process, *Journal of Natural Gas Science and Engineering,* **31**, 589-595.

Zhang Z., Cai J.C., Chen F., Li H., Zhang W.X. and Qi W.J. (2018), Progress in enhancement of CO_2 absorption by nanofluids: A mini review of mechanisms and current status, *Renewable Energy,* **118**, 527-535.

Zhang Z., Chen F., Rezakazemi M., Zhang W.X., Lu C. F., Chang H.X. and Quan X.J. (2017), Modeling of a CO_2-piperazine-membrane absorption system, *Chemical Engineering Research and Design,* 10.1016/j.cherd.2017.11.024.

Zhang Z., Yan Y., Wood D. A., Zhang W., Li L., Zhang L. and Van der Bruggen B. (2015), Influence of the Membrane Module Geometry on SO_2 Removal: A Numerical Study, *Industrial & Engineering Chemistry Research,* **54**, 11619-11627.

Zhang Z.E., Yan Y.F., Zhang L. and Ju S.X. (2014), Hollow fiber membrane contactor absorption of CO_2 from the flue gas: Review and perspective, *Global NEST Journal,* **16**, 355-374.

Zhang Z., Yan Y., Zhang L., Chen Y., Ran J., Pu G. and Qin C. (2014a), Theoretical study on CO_2 absorption from biogas by membrane contactors: Effect of operating parameters, *Industrial & Engineering Chemistry Research,* **53**, 14075-14083.